A simulation of doping and trap effects on the spectral response of AlGaN ultraviolet detectors

Sidi Ould Saad Hamady†

LMOPS, University Paul Verlaine–Metz and SUPELEC–2 Rue Edouard Belin, 57070 Metz, France

Abstract: We study, by means of numerical simulation, the impact of doping and traps on the performance of the "solar blind" ultraviolet Schottky detector based on AlGaN. We implemented physical models and AlGaN material properties taken from the literature, or from the interpolation between the binary materials (GaN and AlN) weighted by the mole fractions. We found that doping and traps highly impact the spectral response of the device, and in particular a compromise in the doping concentration must be reached in order to optimize the spectral response of the detector. These results give us a powerful tool to quantitatively understand the impact of elaboration and processing conditions on photodetector characteristics, and thus identify the key issues for the development of the technology.

Key words: simulation; AlGaN; ultraviolet detector; spectral response

DOI: 10.1088/1674-4926/33/3/034002 **PACC:** 0670D; 2940P; 7280E

1. Introduction

AlGaN-based alloys have attracted a lot of attention and research efforts for ultraviolet (UV) detection because of their attractive physical and electrical properties, such as a sensitivity to only short wavelengths (200 to 350 nm), resistance to ionizing radiation and capacity to operate at high temperature[1].

Despite the technological advances in AlGaN-based detectors, the spectral responses are far from fully optimized and the impact of the device parameters, including the active layer physical parameters–mainly the doping level and trap density–are not well understood and quantified. Some published simulation results were performed with a one-dimensional device structure[2, 3], but suffer from at least two limitations: the impact of the detector geometry cannot be rigorously calculated, and the results are valid only in a restricted range of the physical parameters of the device (i.e. doping). On the other hand, the simulation results obtained with the III-N UV detector device structure do not include the published experimental parameters, in particular the measured absorption coefficient and refractive index spectra, the bandgap, and the mobility and trap properties as input into the simulator. Taking these experimental parameters into account is necessary in order to (i) give a precise description of the device operation; (ii) to understand the physics of the device; and (iii) to give usable feedback for device processing and elaboration for real device optimization.

This paper introduces the device structure, the physical model and parameters used in the simulation, and presents a detailed analysis and discussion of the impact of doping and traps on AlGaN detector performance.

2. The device and the physical model

2.1. The device

Figure 1 shows the device structure of the $Al_{0.26}Ga_{0.74}N$-based UV detector illuminated through the top surface. Gold is used as the Schottky contact and aluminum as the ohmic contact.

In order to have a precise and realistic description of device operation, and hence permit a better understanding of the device physics and optimization of the final detector, the simulator takes as its input the experimental and published optoelectronic properties, such as the refractive index and absorption spectra, the bandgap and mobility physical models, and the trap parameters. Table 1 gives the main parameters used for the AlGaN layer, and Figure 2 shows the gold optical index spectra. In Fig. 3 the experimental refractive index and extinction coefficient spectra of $Al_{0.26}Ga_{0.74}N$ are plotted.

Other parameters (refractive index and absorption spectra, mobility model, Auger recombination, Shockley–Read–Hall (SRH) recombination, etc.) are taken from published experimental works or extrapolated using the bowing parameters.

2.2. Modeling

To simulate the UV detector described in the previous subsection, we used the Silvaco Athena and Atlas tools.

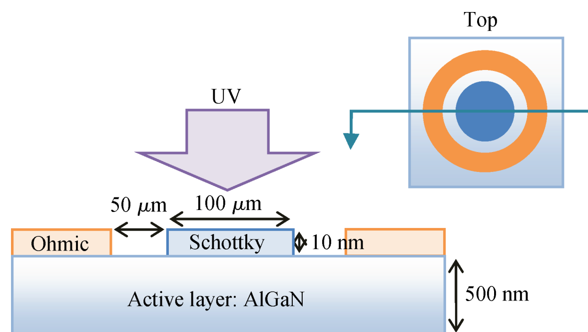

Fig. 1. The structure of the Schottky UV detector.

† Corresponding author. Email: sidi@univ-metz.fr
Received 1 September 2011, revised manuscript received 18 October 2011
© 2012 Chinese Institute of Electronics

Table 1. The AlGaN parameters used in the simulations.

Parameter	Value
Bandgap (eV)	3.95[4]
Electron mobility μ_n ($cm^2/(V\cdot s)$)	200
N-type doping (cm^{-3})	10^{13} – 10^{19}
Thickness (μm)	0.5

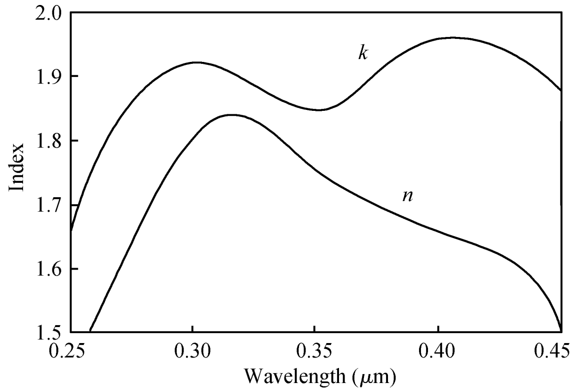

Fig. 2. Gold refractive index (n) and extinction coefficient (k) spectra in the UV spectral region [from www.ioffe.ru/SVA/NSM/nk/index.html].

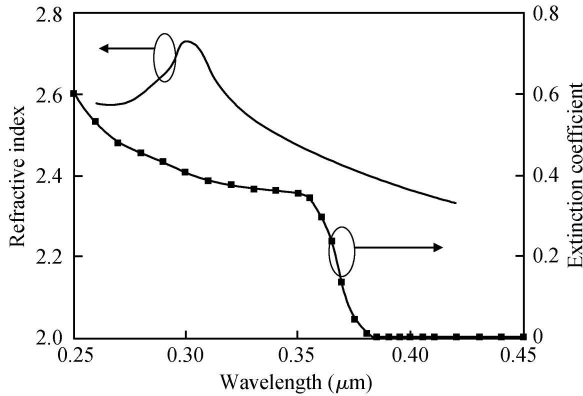

Fig. 3. Refractive index and extinction coefficient spectra of $Al_{0.26}Ga_{0.74}N$. These spectra are extracted from transmission measurements[5].

Athena simulates device processing, including diffusion, etching, metal deposition and lithography, while Atlas solves the 2D coupled continuity and Poisson's equations (Eqs. (1)–(3)) to analyze the device transport properties.

Poisson's equation:

$$\mathrm{div}(\varepsilon \nabla \psi) = -\rho, \tag{1}$$

Continuity equation:

$$\begin{cases} \dfrac{\partial n}{\partial t} = \dfrac{1}{q}\mathrm{div}\boldsymbol{J}_\mathrm{n} + G_\mathrm{n} - R_\mathrm{n}, \\ \dfrac{\partial p}{\partial t} = -\dfrac{1}{q}\mathrm{div}\boldsymbol{J}_\mathrm{p} + G_\mathrm{p} - R_\mathrm{p}, \end{cases} \tag{2}$$

Electron and hole current in the drift–diffusion model:

$$\begin{cases} J_\mathrm{n} = qn\mu_\mathrm{n}\boldsymbol{E}_\mathrm{n} + qD_\mathrm{n} + qD_\mathrm{n}\nabla n, \\ J_\mathrm{p} = qp\mu_\mathrm{p}\boldsymbol{E}_\mathrm{p} - qD_\mathrm{p}\nabla p, \end{cases} \tag{3}$$

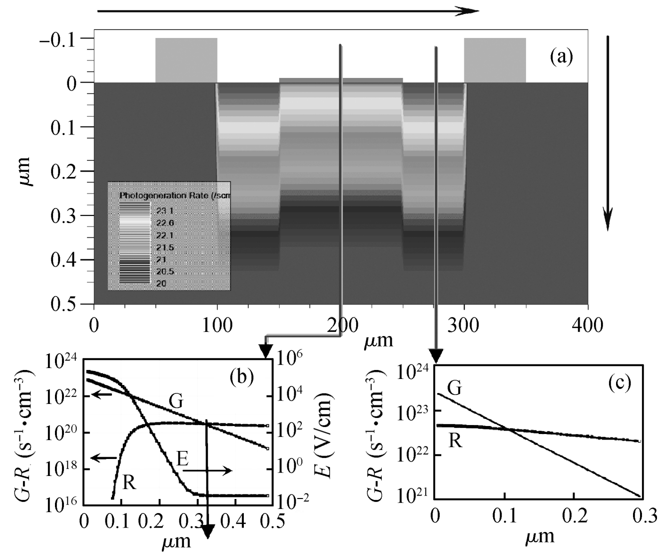

Fig. 4. Photogeneration distribution in the AlGaN UV detector, in log scale (a) and cutlines in the z-direction representing the photogeneration rate G, recombination rate R and electric field E in the two main device regions: under the Schottky contact (b) and between the Schottky contact and the ohmic contact (c). The doping concentration was $N_\mathrm{D} = 10^{16}$ cm^{-3}, and the incident light wavelength $\lambda = 260$ nm.

The Poisson equation includes the densities of electrons, holes and traps with any user-defined distribution. The generation term in the continuity equations represents the optical generation and depends on the active layer refractive index and absorption coefficient spectra, while the recombination term take into account the well-known Auger, band-to-band and trap assisted processes.

3. Results and discussion

The optoelectronic properties of the structure of the detector, described in Section 2.1, were simulated with respect to the n-type doping concentration N_D (from 10^{13} to 10^{19} cm^{-3}) and trap density N_T (from 10^{15} to 10^{17} cm^{-3}). The analyzed output parameters were mainly the electric field, photogeneration and recombination distributions, and the quantum efficiency spectrum.

3.1. Doping

Figure 4 plots the photogeneration distribution in the detector and the variation of photogeneration rate G, recombination rate R and electric field E under the Schottky contact (region b) and in the region not covered by this contact (region c), for a doping concentration of $N_\mathrm{D} = 10^{16}$ cm^{-3}. These three parameters, G, R and E, are obviously of great importance for the photocurrent.

Figure 5 shows the electric field variation perpendicularly to the incident light (in the x-direction) for different doping concentrations. For a low doping concentration, the electric field varies strongly in the x-direction with a maximum value around the Schottky contact borders.

When increasing the doping concentration, N_D, the electric field increases and becomes quite constant in the space charge

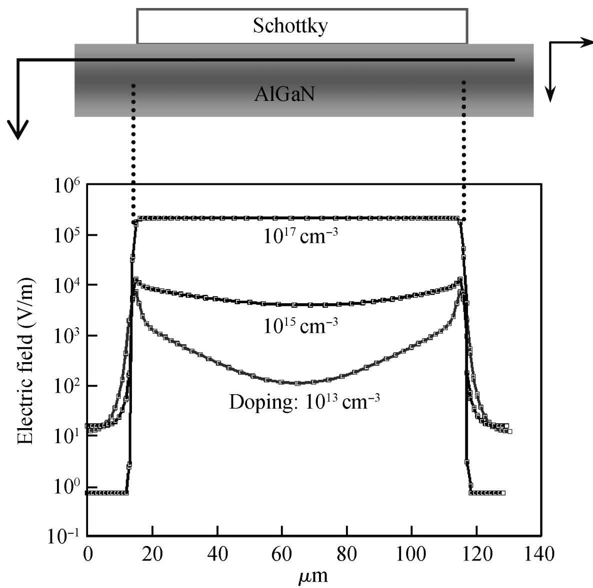

Fig. 5. Electric field (in log scale) versus doping concentration in the active layer, perpendicularly to the incident light (x-direction).

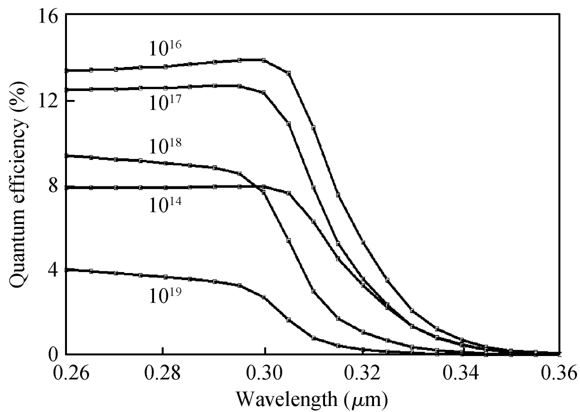

Fig. 6. Quantum efficiency versus doping concentration. The contact thickness is fixed to 10 nm and the width is fixed to 100 μm.

region (SCR), in the x-direction. Figure 6 represents the quantum efficiency spectra versus N_D and Figure 7 shows the variation of the quantum efficiency (QE) value at the wavelength of 260 nm with N_D. The QE increases, up to $N_D = 10^{16}$ cm^{-3}, and then decreases. The optimized QE is obtained for N_D at around 10^{16} cm^{-3}. The highest calculated QE, approximately 13%, is comparable to the highest experimental value usually obtained for an AlGaN detector at zero bias[6].

The increase in doping concentration induces:

(1) an increase in the built-in electric field under the Schottky contact;

(2) a decrease in the SCR width and a decrease in the effective thickness t_{eff}. t_{eff} is defined as the position where the photogeneration rate becomes equal to the recombination rate, as shown in Fig. 4(b);

(3) a change in the ratio between the value of the electric field around the border of the SCR (at $x = 15$ μm in Fig. 4) and in the middle (at $x = 65$ μm in Fig. 4). This ratio, named here as γ, is close to the unity for $N_D = 10^{19}$ cm^{-3} and close to 100 for $N_D = 10^{13}$ cm^{-3}.

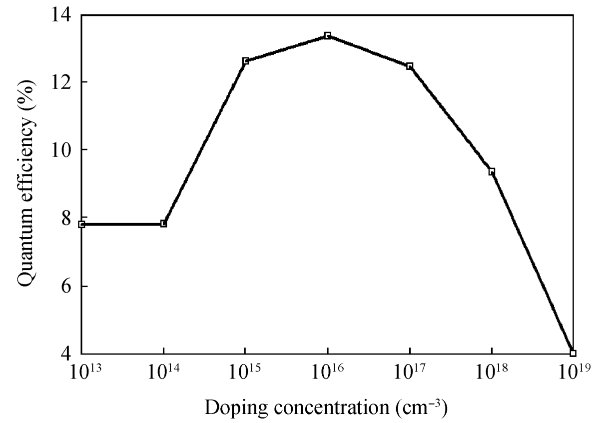

Fig. 7. Quantum efficiency value at the wavelength of 260 nm versus doping concentration.

Table 2. Trap parameters[7].

Parameter	Value
Type	Acceptor
Activation energy (eV, relatively to the valence band)	0.35
Concentration (cm^{-3})	10^{14} – 10^{16}
Electron capture cross section (cm^2)	10^{-19} – 10^{-14}
Hole capture cross section (cm^2)	10^{-19} – 10^{-14}

The above scheme explains the existence of an optimal doping concentration for the detector: the increase in the electrical field induces an improvement in the spectral response, but the decrease in the SCR width counterbalances this improvement. On the other hand, the ratio γ defined above plays an important role in the detector spectral response since the photogeneration rate is higher close to the border (and in the region c) than inside the SCR (region b), and then the higher electric field in this region c impacts more positively the detector photocurrent. The optimal doping concentration found here depends on the contact semi-transparency: if the contact thickness is relatively small, the optimal doping concentration is higher. One can then counterbalance the contact semi-transparency effect by the control of the active layer doping level. This result can be used in the device elaboration process in order to optimize the detector spectral response. Indeed it is experimentally difficult to achieve a high-quality semi-transparent Schottky contact in the UV region, and one can counterbalance the lack of contact transparency by modulating the doping level according to the simulation results.

3.2. Traps

In order to study the role that traps may play in AlGaN detector performance, we include in the simulation one of the main deep traps experimentally studied in Ref. [7]. Table 2 gives the main parameters of this trap, taken as uniformly distributed in the active layer.

Figure 8 plots the quantum efficiency for different trap concentrations. The doping concentration is fixed to its optimal value, calculated above: $N_D = 10^{16}$ cm^{-3}. Figure 9 shows the variation of the quantum efficiency value at the wavelength of 260 nm with respect to trap concentration. We observe that

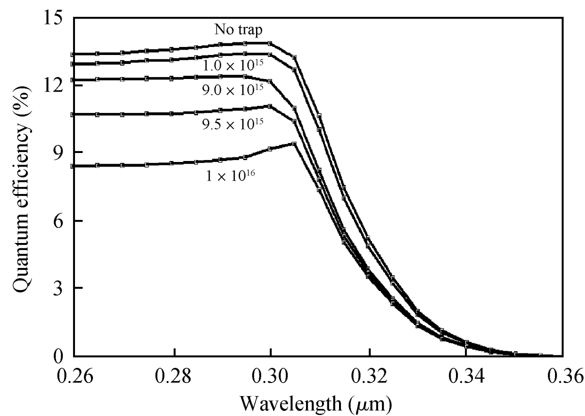

Fig. 8. Quantum efficiency spectra for different trap concentration in the active layer. The doping concentration is equal to 10^{16} cm^{-3}.

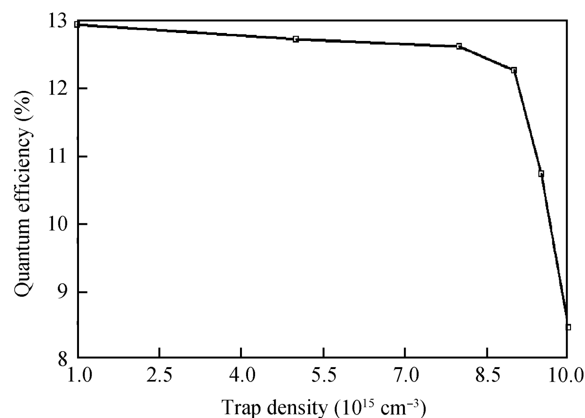

Fig. 9. Quantum efficiency at the wavelength of 260 nm versus trap concentration in the active layer. The doping concentration is equal to 10^{16} cm^{-3}.

the detector quantum efficiency remains almost unchanged as long as the traps concentration is smaller than the doping concentration. When the trap concentration becomes comparable to the doping concentration, the quantum efficiency dramatically decreases.

The direct consequence of this result is that the deep trap concentration must be kept lower, but not necessarily much lower than the free carrier concentration. This means that lowering the doping concentration, in order to optimize the spectral response as shown above, must be accompanied with a decrease in trap density. A compromise must then be found since the defect density remains relatively high in the III-N materials and cannot be arbitrary lowered.

4. Conclusion

In this paper we studied, by means of numerical simulations, the impact of doping and traps on UV "solar blind" Schottky AlGaN detectors. We show that the doping and traps highly impact the spectral response of the device, and, in particular, a compromise in the doping concentration must be reached in order to maximize detector performance. This precise and realistic numerical simulation gives us a powerful tool to quantify and understand the effects of the main device parameters, including the active layer electronic properties.

References

[1] Aslam S. External quantum efficiency of Pt/n-GaN Schottky diodes in the spectral range 5–500 nm. Nucl Instr Meth Phys Res A, 2005, 539: 84

[2] Bouhdadaa A, Hanzaz M, Gibart P, et al. Modeling of the spectral response of $Al_xGa_{1-x}N$ Schottky ultraviolet photodetectors. J Appl Phys, 2000, 87: 8286

[3] Zhou M, Zhao D G. Performance improvement of GaN based Schottky barrier ultraviolet photodetector by adding a thin AlGaN window layer. Chin Phys Lett, 2007, 24: 1745

[4] Nepal N, Li J, Nakarmi M L, et al. Temperature and compositional dependence of the energy band gap of AlGaN alloys. Appl Phys Lett, 2005, 87: 242104

[5] Balmer R S, Pickering C, Kier A M, et al. *In situ* optical monitoring of AlGaN thickness and composition during MOVPE growth of AlGaN/GaN microwave HFETs. J Cryst Growth, 2001, 230: 361

[6] Ozbay E, Biyikli N, Kimukin I, et al. High-performance solar-blind photodetectors based on $Al_xGa_{1-x}N$ heterostructures. IEEE J Sel Topics Quantum Electron, 2004, 10(4): 742

[7] Polyakov A Y, Smirnov N B, Govorkov A V, et al. Deep centers in AlGaN-based light emitting diode structures. Solid-State Electron, 1999, 43: 1929

[8] Wetzel C, Suski T, Ager III J W, et al. Pressure induced deep gap state of oxygen in GaN. Phys Rev Lett, 1997, 78: 3923

[9] Suski T, Perlin P. In: Pankove J I, Moustakas T D, ed. Gallium nitride (GaN) I 50. San Diego: Academic Press, 1998: 279